Virchows Arch (1998) 432:7–16

ORIGINAL ARTICLE

Monique E. De Paepe · Konstantinos Papadakis
Brian D. Johnson · Francois I. Luks

Fate of the type II pneumocyte following tracheal occlusion in utero: a time-course study in fetal sheep

Received: 30 April 1997 / Accepted: 10 July 1997

Abstract Tracheal occlusion in utero has been shown to cause accelerated fetal lung growth and is now being considered as a therapeutic modality for pulmonary hypoplasia. We report the effects of tracheal ligation on the surfactant-producing type II pneumocyte population. Three groups of fetal lambs underwent tracheal ligation of 2 weeks', 4 weeks' and 6 weeks' duration, respectively, and all were sacrificed at 136 days' gestation (9 days pre-term). Nonoperated twins served as controls. The type II pneumocyte population was studied morphometrically using a combination of anti-surfactant protein B immunohistochemistry and computer-assisted stereologic morphometry at light and electron microscopic levels. Single-factor ANOVA was used for statistical analysis. Two weeks of tracheal ligation resulted in doubling of the total lung volume as a result of airspace distension and, to lesser extent, growth of the tissue compartment. With increasing duration of tracheal ligation, there was no additional lung growth. However, more prolonged tracheal occlusion was found to result in significant reduction of the surfactant system, as reflected in the marked decrease of total pneumocyte type II volume (3.14 cm^3, 0.95 cm^3, and 0.46 cm^3, after 2, 4, and 6 weeks of ligation, compared with 5.96 cm^3 for controls) and total pneumocyte type II number (13.9×10^9, 3.8×10^9, and 2.4×10^9, compared with 53.2×10^9 for controls). Ultrastructural analysis of the type II cells in obstructed lungs showed vacuolar degenerative changes that, after 6 weeks of ligation, were apparently irreversible. In utero tracheal ligation causes fetal lung hyperplasia, but results in reduction of and injury to the surfactant-producing cell population. Before tracheal occlusion can find widespread clinical application, its pathophysiology needs to be further elucidated.

Key words Surfactant · Lung development · Lung hypoplasia · Diaphragmatic hernia · Stereology

Presented in part at the 86th Annual Meeting of the United States and Canadian Academy of Pathology, March 1997, Orlando (Fla.)

M.E. De Paepe (✉)
Rhode Island Hospital, Department of Pathology,
593 Eddy Street,
Providence, RI 02903, USA
Tel.: (++1) 401-444-3847, Fax: (++1) 401-444-8514
e-mail 103107.2777@Compuserve.com

K. Papadakis · B.D. Johnson · F.I. Luks
Division of Pediatric Surgery, Rhode Island Hospital and
Brown University School of Medicine,
Providence, R.I., USA

Introduction

Experimental tracheal occlusion in fetal sheep and rabbits has been shown to cause accelerated lung growth before birth [2, 4, 5, 10, 12, 13, 18, 25]. The enhanced lung growth has been ascribed to increased intratracheal pressure, acting in concert with humoral growth factors present in the tracheal fluid [18]. With the development of better techniques for intrauterine surgery [15], tracheal occlusion in utero is now being considered as a therapeutic modality for various forms of pulmonary hypoplasia, mainly for otherwise lethal forms of severe congenital diaphragmatic hernia [25]. Most recently, two centers have reported their initial human experience in treating congenital diaphragmatic hernia-associated pulmonary hypoplasia by tracheal plugging or clipping in the fetus [6, 9].

Before clinical application of in utero tracheal occlusion becomes widespread, it is imperative to elucidate the pathophysiology of lung development induced by tracheal occlusion. Whereas the architectural maturation of obstructed lungs has been studied in detail, little emphasis has been placed on the cellular effects of tracheal occlusion, in particular the effects on the type II pneumocyte population. Type II pneumocytes are of major clinical significance, since these cells are the progenitor of the gas-exchanging type I pneumocyte, produce surfactant, and are the major ion-exchanging cell types [16].

A recent report by O'Toole et al. has demonstrated surfactant deficiencies in obstructed sheep lungs, as suggested by their decreased alveolar phospholipid content

[17]. The aim of the present study is to investigate the effects of varying periods of tracheal occlusion on the development of type II (surfactant-producing) pneumocytes. We analyzed the surfactant system of fetal sheep exposed to 2–6 weeks of tracheal occlusion. To monitor the evolution of the type II pneumocyte population, we applied a morphometric technique based on computer-assisted stereological volumetry in combination with anti-surfactant protein-B immunohistochemical detection of type II cells [22]. Surfactant protein-B has been shown to be expressed early during fetal lung development [14] and is therefore suited for identification and quantitation of type II cells. The morphometric technique was supplemented by transmission and scanning electron microscopic analysis of the type II cells. Our findings confirm that fetal tracheal ligation results in pulmonary hyperplasia. However, this accelerated lung growth is associated with quantitative and qualitative alterations of the type II pneumocyte population that are most dramatic following prolonged (more than 2 weeks) tracheal occlusion.

Methods

Fetal lambs were divided into four experimental groups. Three groups of fetal lambs underwent tracheal occlusion in utero at 122 (n = 5), 108 (n = 3), and 94 (n = 3) days of gestation, respectively (full term=145 days). Non-operated twins served as controls (n = 6). All fetuses were killed near term (day 136; 2, 4 and 6 weeks after ligation, respectively). Tissues were processed for light and electron microscopic morphological and morphometric analysis.

Fetal tracheal ligation was performed in time-dated pregnant ewes. The ewes underwent midline laparotomy under general halothane anesthesia (0.5–2.0% in 100% O_2) after intravenous induction with ketamine (1 g). A small hysterotomy was made transversely near the uterine horn with exteriorization of the fetal head and neck. The uterine wall was secured around the fetal neck with Allis clamps to minimize amniotic fluid loss. The fetal trachea was then exposed and tracheal ligation was performed with a #2 silk suture. The fetal head and neck were returned to the uterus. Antibiotics (ampicillin 200 mg and chloramphenicol 250 mg) were added to the amniotic fluid. The hysterotomy was closed using a two-layer continuous closure, followed by closure of the abdominal wall.

At 136 days' gestation the ewe underwent Cesarean section under the same anesthetic conditions. The previous hysterotomy was utilized to deliver the fetuses. Fetal breathing was prevented by placing a surgical glove over the fetus' head. The fetuses were sacrificed by injection of a euthanasia solution (3 ml of Beuthanasia-D Special, Shering-Plough Animal Health Corp., Kenilworth, N.J.) into an umbilical vein after clamping of the cord.

The fetal body weight was recorded, and the lungs and trachea were removed en bloc. The wet weight of the lungs and attached tracheal stump was determined. After placement of a leak-proof ligature, small tissue samples were removed from the right upper lobe and fixed in Karnovsky's fixative (4% paraformaldehyde, 2.5% glutaraldehyde, 0.1 M sodium cacodylate buffer pH 7.2) for ultrastructural analysis. Fixation of the remainder of the lung was accomplished by tracheal instillation of 10% buffered formaldehyde maintained at a pressure of 25 cm H_2O with the lungs immersed in a beaker containing buffered fixative. The lungs of corresponding twins were fixed in parallel to eliminate fixation variability. After at least 1-week fixation at 21°C, the volume of the lungs was estimated by the volume displacement method [1]. The left lung was cut in standardized sections (3–5 mm thick) and random blocks were taken from the center and periphery of each lobe and embedded in paraffin. Hematoxylin-eosin-stained slides (4 μm thick) were prepared from each paraffin block (4 per animal).

Two sections per lung (central upper lobe, peripheral lower lobe) were processed for avidin–biotin-immunoperoxidase staining using a polyclonal rabbit antibody against surfactant protein B (SP-B). The polyclonal anti-bovine SP-B antiserum was kindly provided by Dr. J.A. Whitsett [22]. After treatment with 3,3'-diaminobenzidine tetrachloride (DAB; Sigma, St. Louis, Mo.), sections were either left unstained (for immunodensitometry) or lightly counterstained with hematoxylin, cleared and mounted. Controls for specificity consisted of omission of the primary antibody.

To estimate the cellular concentration of surfactant protein, the specific absorbance of SP-B-immunostained type II pneumocytes was determined according to well-established methods that make the measure independent of section thickness, nonspecific background, or variations in photometric illumination [19]. To this end, lung sections were immunostained in one session and anti-SP-B antiserum was used at a high dilution to optimize quantitative measurement. To assess the specificity of labelling, the anti-SP-B antibody was omitted. Under these conditions, the optical density of the type II cells was the same as that of the surrounding lung parenchyma.

Total SP-B-immunoreactive volume, as a measure of total pneumocyte type II volume, was determined using standard stereological volumetric techniques [3, 8]. To avoid sampling bias, design-based sampling methods [3] were used throughout the experimental protocol. Tissue sections from the left lung, stained with hematoxylin-eosin or anti-SP-B antibody, were analyzed morphometrically using a computerized image analysis system [Olympus BX-40 microscope (Olympus) interfaced via a CCD video camera (KP-161, Hitachi) to a Power Macintosh 7100/80AV (Apple Corp., Cupertino, Calif.) equipped with software for image analysis (Image NIH 1.59 for Macintosh, National Institutes of Health, Bethesda, Md.)]. The number of fields to be examined for each type of measurement was determined by testing the reproducibility of results in a pilot study. Statistical analysis was performed using the StatView program (StatView, Abacus, Berkeley, Calif.). Data derived from measurements of the left lung were extrapolated to both lungs. The critical data set and hierarchical equations, obtained by examining the lung at increasing levels of magnification, comprised:

Volume of lung: $V(\text{lu})$
Volume of parenchyma: $V(\text{pa})$
$V(\text{pa}) = A_A(\text{pa/lu}) \times V(\text{lu}) = 0.9 \times V(\text{lu})$
Volume of air-exchanging parenchyma: $V(\text{ae})$
$V(\text{ae}) = A_A(\text{ae/pa}) \times V(\text{pa})$
Volume of surfactant-positive (type II) compartment: $V(\text{pnII})$
$V(\text{pnII}) = A_A(\text{pnII}/ae) \times V(\text{ae})$
Volume of surfactant-positive (type II) cell: $V(\text{pnIIcell})$
$V(\text{pnIIcell}) = 4/3\ \pi\ r^3$
Total number of type II pneumocytes per lung:
$\#\text{pnII} = V(\text{pnII})/V(\text{pnIIcell})$

Volume of lung

The volume of fixed lung was determined according to the Archimedes principle [1]. As the lungs of experimental and control animals were processed identically, no correction was made for dehydration and embedding.

Volume of parenchyma

Subsequent steps in the structural hierarchy involved point counting methods based on computer-assisted image analysis. The parenchymal areal density was estimated by dividing the number of points falling on parenchyma (lung excluding large bronchi and blood vessels) by the number of points falling on the entire lung (magnification 10×). In a pilot study, the parenchymal areal densi-

ty consistently approached 90 ± 2% in all experimental groups. V(pa) was subsequently estimated by multiplying V(lu) by 0.9.

Volume of air-exchanging parenchyma

The areal density of air-exchanging parenchyma [A_A(ae/pa)], which represents the parenchymal tissue fraction was estimated by studying random fields of peripheral lung parenchyma and dividing the number of points falling on air-exchanging parenchyma (peripheral lung parenchyma excluding airspace) by the number of points falling on the entire field (tissue and airspace) (magnification 100×). The optical density of air-exchanging parenchyma differed sufficiently from that of air spaces to allow automatization of this procedure. The total volume of air exchanging parenchyma was calculated by multiplying its areal density by the parenchymal volume. A_A(ae/pa) represents the tissue fraction of the lung, and as such is inversely related to the air space fraction (ASF), a traditional measure of fetal lung maturation [A_A(ae/pa) = 1-ASF].

Volume of surfactant-positive (type II) compartment

To determine the areal density of the SP-B-immunoreactive compartment, sections immunostained with anti-SP-B antibodies and lightly counterstained with hematoxylin were used (magnification 200×). For each section the illumination was optimized by Koehler illumination, and the light intensity was standardized by calibration of the threshold using endothelial cell (surfactant-negative) cytoplasm as standard. Based on the fact that the immunohistochemical staining of type II cells produces a higher grey level than that of the background, the surfactant-positive area was evaluated automatically. To maximize the detection of type II cells with low surfactant content, the primary antibody was used at high concentration and the grey level threshold was interactively adjusted when indicated. The operator was blinded with respect to the source of the tissues.

Individual volume of surfactant-positive (type II) cell

To determine the individual pneumocyte II profile area, surfactant-positive cells were manually traced at a final magnification of 600× and their profile area and radius (r) determined. At least 50 pneumocytes per animal were analyzed, from 5 different microscope fields. The individual pneumocyte II volume was calculated by the following formula, based on the observation that the shape of type II pneumocytes approaches a spherical configuration: V(pnIIcell) = 4/3 π r^3.

Total number of type II pneumocytes per lung

The total number of type II pneumocytes per lung was calculated by dividing the total pneumocyte II volume [V(pnII)] by the individual pneumocyte II volume [V(pnIIcell)].

For transmission electron microscopy, lung tissue fragments were fixed in Karnovsky's fixative, osmicated, dehydrated in ethanol, and embedded in epoxy-resin. Ultrathin sections of blocks that did not contain large blood vessels or airways were stained with uranyl acetate and lead citrate, and examined with a Philips 301 electron microscope operated at 60 kV. Sections were prepared from two randomly selected blocks from fetuses of groups II and III (4 weeks' ligation and controls).

Type II pneumocytes were defined by the presence of microvilli and lamellar bodies. The first ten type II cells observed in the right upper corner of a section-covered grid hole were photographed at a constant magnification (7,500×). Analysis was limited to those cells in which the nucleus was sectioned. Bias was avoided in the selection of cells to be photographed by the coding of the grids and by systematic scanning of each grid. The negatives were printed at a constant enlargement (final magnification 24,000×), and analyzed using morphometric methods [20, 23]. The electron micrographs were evaluated using a flatbed scanner (Scanmaker E3, Microtek, Redondo Beach, Calif.) interfaced to image analysis software (Image NIH). The profile area of each cell [A(cell)] and its nucleus were determined by planimetry. The areal density of the nucleus [A_A(nucl/cell)] was estimated by dividing the number of points falling on nucleus by those falling on cell [ΣP(nucl)/ΣP(cell) (%)]. The profile areas of lamellar bodies within each cell were also measured by planimetry. The areal density of lamellar bodies [A_A(lambod/cell)] was calculated by dividing the sum of points falling on lamellar bodies by the number of points falling on cell cytoplasm (cytoplasmic area = whole cell area – nucleus area) [ΣP(lambod)/ΣP(cyto) (%)].

For scanning electron microscopy, formaldehyde-fixed lung samples were post-fixed in Karnovsky's fixative, dehydrated in a graded acetone series, and critical-point-dried with liquid CO_2. Samples were partially cut with a razor blade and then pulled apart to reveal fractured surfaces free of cutting and compression artifacts. Specimens were glued to aluminum stubs and sputter coated with a thin layer of gold/palladium prior to examination at 15 kV with a Philips 515 scanning electron microscope (Philips Electronics, Mahwah, N.J.). Digital images were acquired using the PGT/IMIX (Princeton Gamma Tech Inc., Princeton, N.J.) digital interface system and printed on a Codonics dye sublimation printer (Codonics, Middleburg Heights, Ohio).

Statistical analysis was performed using single-factor analysis of variance (ANOVA) for comparison of four nonparametric groups. Where appropriate, values are expressed as mean ± standard deviation (SD). A P-value < 0.05 was considered statistically significant. All procedures and protocols were approved by the Brown University Animal Care and Use Committee and in accordance with standard principles of laboratory animal care (NIH publication no. 85-23, revised 1985).

Results

Fetal body weights were similar in all experimental groups studied (Table 1). The ratio of lung weight normalized to body weight (LW/BW) increased two-fold after 2 weeks of ligation. LW/BW was comparable after 2, 4 and 6 weeks' ligation (Table 1).

The lungs of control fetuses were divided into small, regular alveolar units (Fig. 1A). The bronchioles were easily recognizable and opened into relatively short and inconspicuous alveolar ducts. The alveoli appeared well defined by prominent alveolar septa (Fig. 1A). In obstructed lungs, the future air spaces were more dilated, with associated attenuation of the septa and flattening of the crests (Fig. 1B, C). The air space dilatation appeared more prominent after 4 and 6 weeks than after 2 weeks

Table 1 Lung and body weight. Values shown are mean±SD obtained in (n) animals

	Control (6)	2 week ligation (5)	4 week ligation (3)	6 week ligation (3)
Body wt. (kg)	3.68±0.59	4.00±0.69	3.67±0.73	3.59±0.81
Lung wt/Body wt. (%)	4.72±0.54	9.25±2.45*	9.49±2.74**	9.83±2.16**

* P<0.02; ** P<0.01 versus control (other differences not statistically significant)

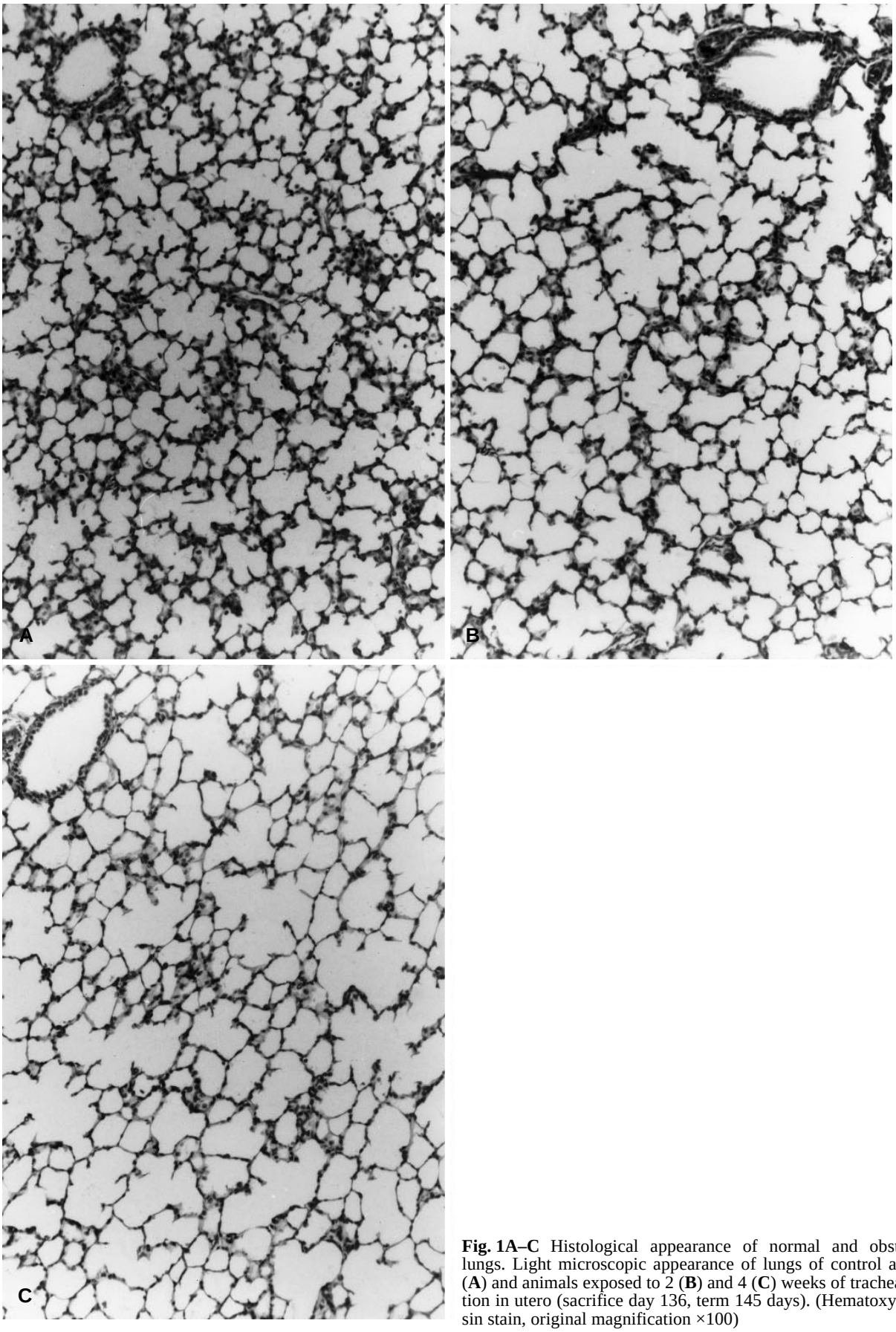

Fig. 1A–C Histological appearance of normal and obstructed lungs. Light microscopic appearance of lungs of control animals (**A**) and animals exposed to 2 (**B**) and 4 (**C**) weeks of tracheal ligation in utero (sacrifice day 136, term 145 days). (Hematoxylin-eosin stain, original magnification ×100)

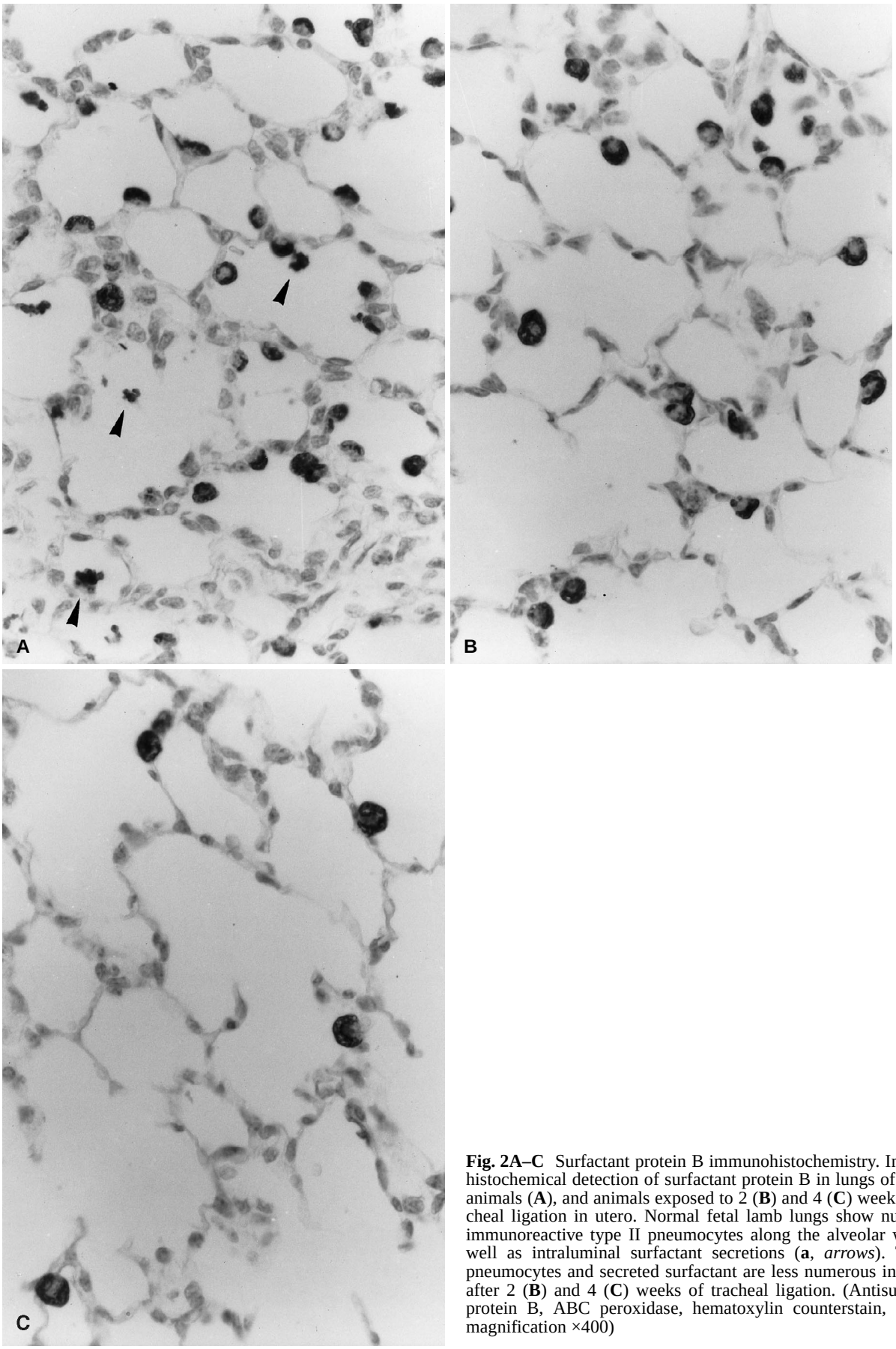

Fig. 2A–C Surfactant protein B immunohistochemistry. Immunohistochemical detection of surfactant protein B in lungs of control animals (**A**), and animals exposed to 2 (**B**) and 4 (**C**) weeks of tracheal ligation in utero. Normal fetal lamb lungs show numerous immunoreactive type II pneumocytes along the alveolar walls as well as intraluminal surfactant secretions (**a**, *arrows*). Type II pneumocytes and secreted surfactant are less numerous in fetuses after 2 (**B**) and 4 (**C**) weeks of tracheal ligation. (Antisurfactant protein B, ABC peroxidase, hematoxylin counterstain, original magnification ×400)

Table 2 Stereological morphometry (light microscopy). Values shown are mean±SD in (*n*) animals (*V (lu)* lung volume, *V (pa)* parenchymal volume, A_A *(ae/pa)* areal density of air exchanging parenchyma, *V (ae)* volume of air exchanging parenchyma)

	Control (6)	2-week ligation (5)	4-week ligation (3)	6-week ligation (3)
V (lu) (cm^3)	177±39	362±85†	345±90†	364±75†
V (pa) (cm^3)	159±33	326±77††	310±75††	328±57††
A_A (ae/pa) (%)	29.3±3.4	24.4±1.9*	20.6±0.6†	18.8±2.4††
V (ae) (cm^3)	46.6±7.2	79.5±20.3††	63.9±13.4*	61.7±14.6*
Specific Absorbance	0.22±0.05	0.27±0.06	0.32±0.04*	0.33±0.07*

* $P<0.05$; † $P<0.01$; †† $P<0.02$ versus control

of ligation. The bronchi and vascular structures appeared similar in all experimental groups.

Anti-SP-B immunohistochemistry revealed positive staining in type II cells as well as in nonciliated bronchiolar (Clara) cells. In control animals, type II pneumocytes appeared to be relatively abundant; usually one or two type II cells were seen in each primitive airspace (Fig. 2A). Numerous type II cells showed apical surfactant-positive aggregates adherent to the cell, interpreted as actively secreted surfactant. In addition, many future air spaces displayed coarsely granular immunoreactive deposits, representing recently secreted surfactant (Fig. 2A). In ligated animals, the lungs showed a relative paucity of anti-SP-B immunoreactive cells (Fig. 2B, C), which was more striking after 4 and 6 weeks' ligation. Furthermore, the staining in ligated animals appeared to be more intense than that in control animals. Whereas following 2 weeks' ligation, lungs still showed rare luminal surfactant deposits, no immunoreactive surfactant was observed in the air spaces of lungs following more prolonged ligation.

The impression of increased SP-B immunoreactivity in obstructed lungs was confirmed by the quantitative determination of the specific absorbance. The specific absorbance of type II cells, reflecting their cellular surfactant content, was significantly higher in obstructed lungs than in control animals (Table 2).

Two weeks of tracheal obstruction resulted in a doubling of the total lung volume [*V*(lu)] (Table 2). Interestingly, no additional increase in lung volume was seen in lungs that had been obstructed for 4 or 6 weeks. The areal density of air exchanging parenchyma [A_A(ae/pa)] showed a progressive decrease in obstructed lungs, i.e., the air space fraction [1 – A_A(ae/pa)] progressively increased following ligation. The total volume of air exchanging parenchyma [*V*(ae)], which takes into account both *V*(pa) and A_A(ae/pa), significantly increased after 2 weeks' ligation. There was no further increase in *V*(ae) in lungs that had been exposed to 4 or 6 weeks' ligation. The relative contribution of *V*(ae) to *V*(pa) was found to be smaller in ligated fetuses than in controls, indicating that distension of air spaces, rather than actual tissue growth, was proportionally more important in causing the lung expansion.

The total type II cell volume [*V*(pnII)] showed a twofold reduction following 2 weeks of ligation and a more than 6-fold reduction following 4 and 6 weeks' ligation (3.14 ± 2.38 cm^3 after 2 weeks' ligation, 0.95 ± 0.19 cm^3 after 4 weeks' ligation, 0.46 ± 0.18 cm^3 after 6 weeks' ligation, versus 5.96 ± 2.98 cm^3 in control fetuses; Fig. 3A). The individual cell volume [*V*(pnIIcell)] of type II cells in obstructed lungs showed a 100% increase compared with control fetuses (225.1 ± 51.4 μm^3 after 2 weeks' ligation, 247.8 ± 94.2 μm^3 after 4 weeks' ligation, 256.5 ± 84.3 μm^3 after 6 weeks' ligation, versus 112.2 ± 23.3 μm^3 in control fetuses; Fig. 3B). Dividing *V*(pnII) by *V*(pnIIcell) to estimate the total pneumocyte II number per lung (#pnII), revealed a profound reduction of the type II pneumocyte population following ligation (from 53.2×10^9 in control animals to 13.9×10^9 after 2 weeks' ligation and 2.4×10^9 after 6 weeks' ligation; Fig. 3C).

The air-exchanging parenchyma of control lungs revealed a well-preserved architecture on transmission electron microscopy, with relatively cellular and thick alveolar septa. Numerous alveolar type II cells were observed, showing characteristic microvilli and osmiophilic lamellar bodies, and also numerous mitochondria and a prominent endoplasmic reticulum (Fig. 4A). The luminal surface of the cells showed prominent microvillous projections and pit-like depressions suggestive of secretory activity. Whorled and lamellar electron-dense material, consistent with recently secreted surfactant, was frequently observed in the future air spaces (Fig. 4A).

In trachea-ligated lungs, the alveolar septa appeared markedly attenuated. Type II pneumocytes appeared to be infrequent, and larger than those of control lungs (Fig. 4B). The cellular swelling was associated with the accumulation of vacuoles in the cytoplasm, some of which showed poorly preserved lamellar inclusions. The plasma membrane, microvilli and nucleolar complex did not show significant alterations following 2 weeks' ligation. Cytoplasmic degenerative changes were more prominent after 4 weeks' ligation, and after 6 weeks were associated with marked mitochondrial swelling and damage to the cell membranes (not shown). No secreted surfactant was observed in the air spaces. Glycogen pools were not seen in any of the experimental groups at this advanced gestational stage. Morphometric analysis of the electron micrographs revealed marked differences between normal pneumocytes and those of ligated lungs (Table 3). The cellular profile area of type II cells showed a 50% increase following 4 weeks of ligation as compared with controls. The nuclear areal density showed a concomitant 100% decrease. The areal density of presumably surfactant-associated bodies showed a 6-fold increase following ligation (Table 3).

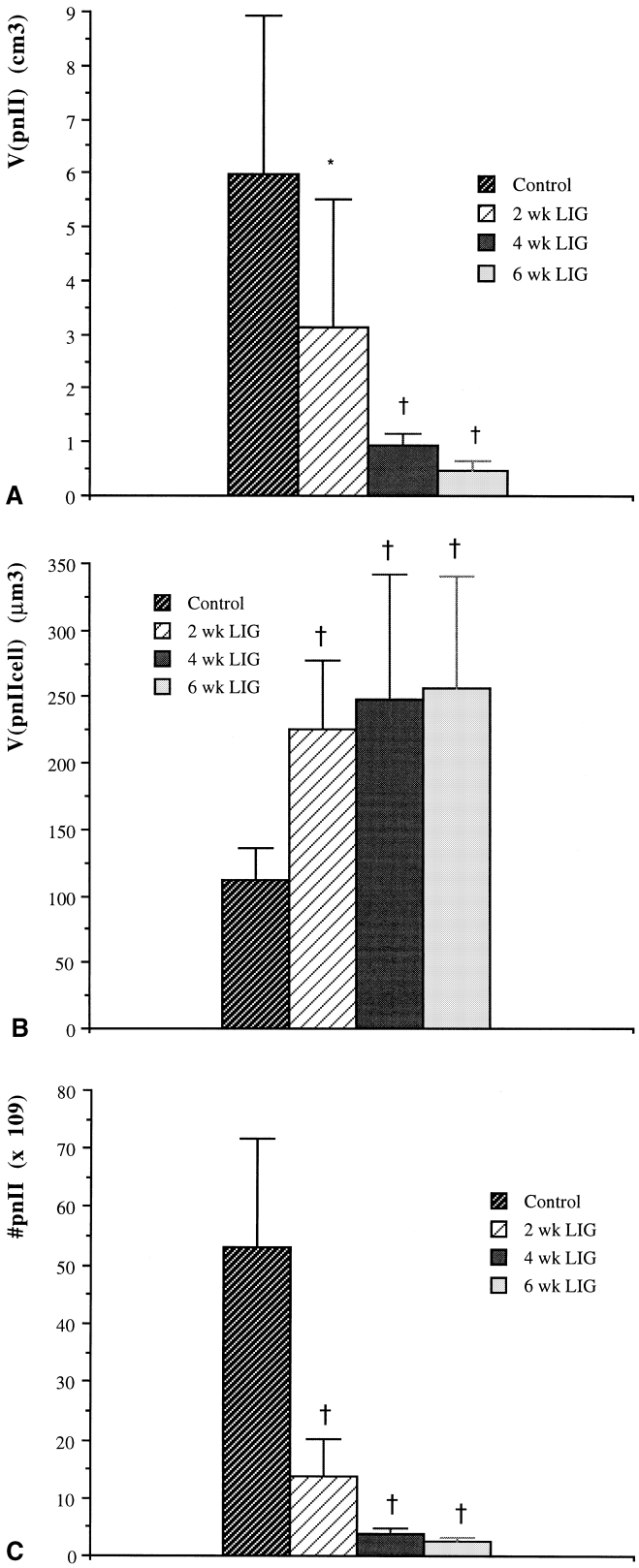

Fig. 3A–C Stereological morphometric analysis of type II cell population (light microscopy). **A** Total volume of type II population [V(pnII)]. **B** Individual volume of type II cell [V(pnIIcell)]. **C** Total number of type II pneumocytes per lung (#pnII). Values depicted represent mean ± SD. *$P < 0.05$ versus controls, †$P < 0.01$ versus controls

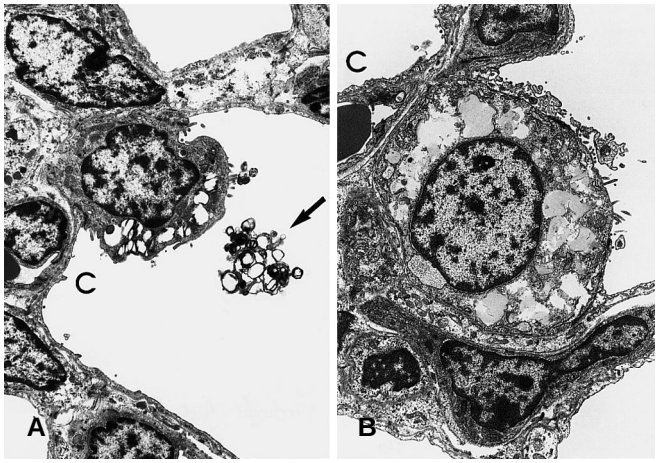

Fig. 4A, B Transmission electron microscopy. Ultrastructural appearance of type II pneumocytes in lungs of control animals (**A**) and animals after 4 weeks of tracheal ligation (**B**). The type II cells contain microvilli and are located in the angulated portion of the air space. In normal fetuses, surfactant-containing bodies are concentrated along the luminal aspect of the type II cell and show distinct lamellation of the surfactant content (**A**). Whorled aggregates of recently secreted surfactant are seen in the lumen of the air space (**A**, *arrow*). The type II cells of obstructed lungs appear enlarged and show vacuolization of the cytoplasm without obvious lamellation (**B**). The mitochondria are enlarged, but the cell membrane and microvilli appear intact. **A**, **B** Taken at the same magnification (*c*, capillary). (Lead citrate and uranyl acetate, final magnification ×8,150)

Table 3 Type II pneumocyte morphometry (electron microscopy). Values shown are mean±SD obtained in (*n*) animals (*A (cell)* profile area of type II cell, A_A*(nucl/cell)* nuclear areal density of type II cell, A_A *(lambod/cell)* areal density of lamellar bodies or (in obstructed lungs) presumably surfactant-associated bodies, *sq px* square pixels)

	Control (3)	4 week ligation (3)
A (cell) (×10^3 sq px)	83.5±10.0	116.1±18.0††
A_A (nucl/cell) (%)	46.5±6.5	24.6±2.4†
A_A (lambod/cell) (%)	6.2±2.4	40.0±3.6†

†P<0.01; ††P<0.02 versus control

In control animals, the lung parenchyma showed regularly distributed alveolar ducts and alveoli, which appeared uniform in size and shape on scanning electron microscopy (Fig. 5A, B). Type II pneumocytes were identified as spherical to cuboidal cells with microvillous projections, protruding from the alveolar wall. On average, each alveolus was found to contain one to three type II pneumocytes. The lung parenchyma of animals 4 weeks after tracheal ligation appeared to be distorted due to a marked enlargement of the alveolar ducts and sacs (Fig. 5C, D). The alveoli varied markedly in size and shape and appeared smooth-walled and much deeper than those of control animals. Only sparse type II pneumocytes were found in the lungs of ligated animals (Fig. 5D).

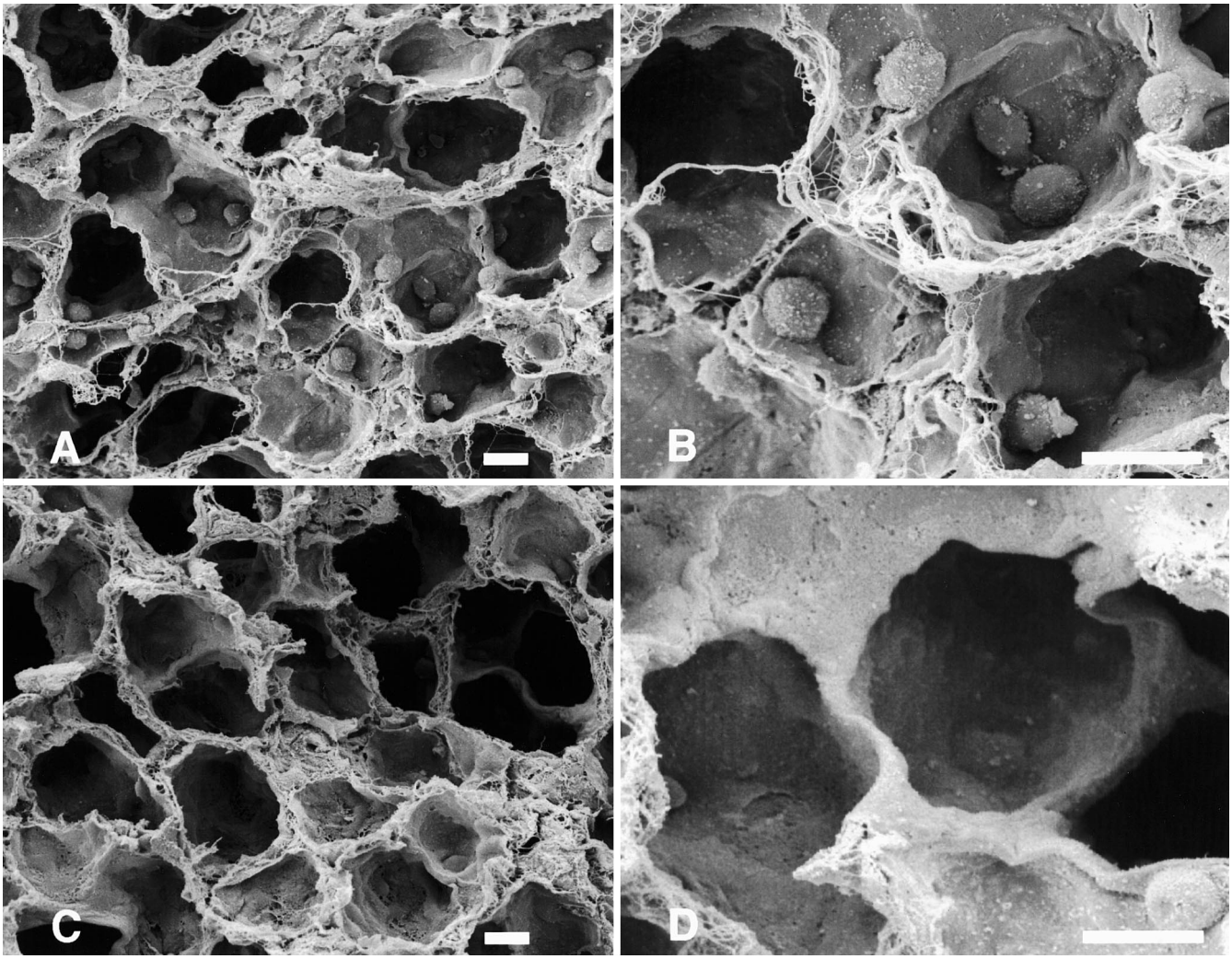

Fig. 5A–D Scanning electron microscopy. Scanning electron micrographs of lungs of control animals (**A**, **B**) and animals after 4 weeks of tracheal ligation (**C**, **D**). The alveolar spaces of normal fetal lungs contain numerous type II cells, easily recognized by their spherical shape and microvillous projections (**A**, **B**). Obstructed lungs show enlarged air spaces (**C**, **D**) with only sparse type II cells (**d**, *bottom right*). (Size bar: 10 μm)

Discussion

The basic architecture of the air exchanging or alveolar region of mammalian lungs is strikingly similar between species. Two types of cells cover the alveolar surface: the type I cell is characterized by attenuated cytoplasm to enhance gas exchange, and the type II cell is cuboidal to spherical, frequently found in the angulated portion of the alveolus, and characterized by an abundance of microvilli on the alveolar surface and osmiophilic lamellar inclusion bodies which contain pulmonary surfactant. Type I cells cover the largest area, approximately 95% of the alveolar surface area, whereas type II cells, which are almost twice as abundant, have a much smaller size.

Alveolar type II cells synthesize and secrete pulmonary surfactant, a surface-active material composed of phospholipid-rich lipoproteins that reduces surface tension at the alveolar surface, promoting lung expansion on inspiration and preventing lung collapse on expiration [11]. The importance of a functioning surfactant system to lung function is clearly demonstrated by the acute respiratory failure due to atelectasis that complicates premature birth before maturation of the surfactant system, and the dramatic response of these infants to intratracheally instilled exogenous surfactant.

Little is known about the fate of the surfactant system in fetal lungs that have been subjected to tracheal occlusion. This procedure, known to promote lung growth in utero, has been advocated – and applied – as a therapeutic measure in severe forms of congenital diaphragmatic hernia (CDH) [6, 9, 12, 25]. Congenital diaphragmatic hernia in itself is associated with surfactant deficiency [7, 21, 24]. Hence, if tracheal occlusion in utero is to be used in this setting, the effect of tracheal obstruction on type II cells is of critical importance.

In the present study, we report a stereological morphometric analysis of the effect of varying periods of tracheal occlusion in utero on the type II pneumocyte population. The degree of total lung growth associated with tracheal ligation in this study was similar to that reported

by others [2, 5, 10, 25]: lung weight and volume more than doubled after 2 weeks of tracheal ligation.

Although most of the lung expansion was found to be due to distension of the air spaces, there was also a significant increase of the air-exchanging parenchymal volume. The increase in parenchymal tissue indicates that the lung growth induced by this procedure involves actual growth of the tissue, and not mere passive dilatation as a result of retained lung fluid. Thus, the increased air-exchanging parenchymal volume can be considered to be the morphometric correlate of previously reported increases in total DNA content [10, 25]. The morphometric technique has the advantage of allowing visualization of the tissue under investigation. DNA analysis, in contrast, requires homogenization of the tissue, and variable amounts of extrinsic elements such as passenger leukocytes and hematopoietic cells may contribute to the total pulmonary DNA content.

Interestingly, tracheal occlusion of more than 2 weeks' duration did not result in additional lung growth: both the total lung volume and total air-exchanging parenchymal volume were similar in fetuses exposed to 2, 4, or 6 weeks of ligation. These results suggest that there is no further tissue growth or distension (and, presumably, secretion) after 2 weeks of tracheal occlusion. In the clinical setting, limitation of tracheal occlusion to 2 weeks or less may thus be indicated, in order to promote lung growth without causing adverse effects on the fetal lungs. However, the 2 weeks', 4 weeks' and 6 weeks' ligation groups may not be fully comparable, since they were at different developmental stages at the time of tracheal ligation (122days, 108days, and 94days of gestation, respectively). Whether the gestational age at the time of tracheal occlusion plays a part in the extent of accelerated lung growth awaits further study.

Combination of computer-assisted stereological volumetry with immunohistochemical detection of type II cells using anti-surfactant protein-B antibodies allowed specific monitoring of the surfactant compartment following tracheal occlusion. At the cellular level, tracheal ligation was found to cause profound quantitative and qualitative alterations in the surfactant system. There was a significant reduction of the type II pneumocyte population; both total number and total volume of type II pneumocytes were dramatically decreased. Furthermore, the type II cells of obstructed lungs demonstrated marked morphological alterations, best described as vacuolar degeneration. The cell injury observed may well be related to previously reported in vitro functional deficits of type II cells in obstructed lungs [17]. Several in vivo morphological observations made during our study suggest the existence of a secretory defect. Type II cells of obstructed lungs were engorged with cellular surfactant, and surfactant secretions were conspicuously absent from the air spaces.

It is uncertain to what extent the observed depletion of the type II cell population is attributable to decreased cell proliferation, increased differentiation to type I pneumocytes, or cell death. The reduction of the type II cell population is most probably in large part attributable to accelerated terminal differentiation to type I pneumocytes, induced by stretch. Indeed, the residual type II cells did not display light or electron microscopic evidence of apoptosis (programmed cell death) or necrosis. Type II cells exposed to 6 weeks of tracheal ligation displayed ultrastructural evidence of irreversible cell injury, including extensive damage to plasma membranes and prominent mitochondrial swelling. However, the injury observed following 2 and 4 weeks of ligation appears to be reversible, since the plasma membranes were found to remain intact.

In conclusion, this stereological morphometric study demonstrates significant quantitative and qualitative impairment of the surfactant system in lungs following prolonged tracheal obstruction. If tracheal occlusion is to be used clinically in fetuses with pulmonary hypoplasia who are already exposed to surfactant deficiencies due to their immaturity, the implications and pathogenetic mechanisms of the surfactant depletion need to be further defined experimentally. Stereological morphometry of the type II cell compartment, based on immunohistochemical detection of type II cells in conjunction with computer-assisted stereological morphometry, allows precise quantitation of the surfactant system and is invaluable in monitoring the type II cells under various experimental conditions.

Acknowledgements This study was supported in part by grant no. 5477 from the Rhode Island Foundation. The authors are grateful to Si Lin Sun for excellent histotechnology services, and to Patrick Verdier for scanning electron microscopy.

References

1. Aherne WA, Dunnill MS (1982) The estimation of whole organ volume. In: Aherne WA, Dunnill MS (eds) Morphometry. Arnold, London, pp 10–18
2. Alcorn DA, Adamson TM, Lambert TF, Maloney JE, Ritchie BC, Robinson PM (1977) Morphological effects of chronic tracheal ligation and drainage in the fetal lamb lung. J Anat 123:649–660
3. Bolender RP, Hyde DM, Dehoff RT (1993) Lung morphometry: a new generation of tools and experiments for organ, tissue, cell, and molecular biology. Am J Physiol 265:L521–L548
4. Carmel AJ, Friedman F, Adams FH (1965) Fetal tracheal ligation and lung development. Am J Dis Child 109:452–456
5. Difiore JW, Fauza DO, Slavin R, Peters CA, Fackler JC, Wilson JM (1994) Experimental fetal tracheal ligation reverses the structural and physiological effects of pulmonary hypoplasia in congenital diaphragmatic hernia. J Pediatr Surg 29:248–257
6. Flake AW, Johnson MP, Treadwell M, Mason B, Cauldwell C, Phillipart AI, Cullen ML, O'Brien J, Adzick NS, Harrison MR, Evans MI (1996) In utero treatment of right-sided congenital diaphragmatic hernia (R-CDH) by prenatal tracheal occlusion (abstract). Am J Obstet Gynecol 174: 489
7. Glick PL, Stannard VA, Leach CL, Rossman J, Hosada Y, Morin FC, Cooney DR, Allen JE, Holm B (1992) Pathophysiology of congenital diaphragmatic hernia II: the fetal CDH lamb model is surfactant deficient. J Pediatr Surg 27:382–388
8. Gundersen HJG, Bendtsen TF, Korbo L, Marcussen N, Møller A, Nielsen K, Nyengaard JR, Pakkenberg B, Sørensen FB, Vesterby A, West MJ (1988) Some new, simple and efficient

stereological methods and their use in pathological research and diagnosis. APMIS 96:379–394
9. Harrison MR, Adzick NS, Flake AW, Vanderwall KJ, Beaker JF, Howell LJ, Farrell JA, Filly RA, Rosen MA, Sola A, Goldberg JD (1996) Correction of congenital diaphragmatic hernia in utero VIII: Response of the hypoplastic lung to tracheal occlusion. J Pediatr Surg 31:1339–1348
10. Hashim E, Laberge J-M, Chen M-F, Quillen EW Jr (1995) Reversible tracheal obstruction in the fetal sheep: effects on tracheal fluid pressure and lung growth. J Pediatr Surg 30:1172–1177
11. Hawgood S (1997) Surfactant: composition, structure and metabolism. In: Crystal RG, West JB, Weibel ER, Barnes PJ (eds) The lung. Scientific foundations. Lippincott-Raven, Philadelphia, pp 557–571
12. Hedrick MH, Estes JM, Sullivan KM, Bealer JF, Kitterman JA, Flake AW, Adzick NS, Harrison MR (1994) Plug the lung until it grows (PLUG): a new method to treat congenital diaphragmatic hernia in utero. J Pediatr Surg 29:612–617
13. Lanman JT, Schaffer A, Herod L, Ogawa Y, Castellanos R (1971) Distensibility of the fetal lung with fluid in sheep. Pediatr Res 5:586–590
14. Liley HG, White RT, Warr RG, Benson BJ, Hawgood S, Ballard PL (1989) Regulation of messenger RNAs for the hydrophobic surfactant proteins in human lung. J Clin Invest 83:1191–1197
15. Luks FI, Gilchrist BF, Jackson BT, Piasecki GJ (1996) Endoscopic tracheal obstruction with an expanding device in a fetal lamb model. Fetal Diagn Ther 11:67–71
16. Mason RJ, Shannon JM (1997) Alveolar type II cells. In: Crystal RG, West JB, Weibel ER, Barnes PJ (eds) The lung. Scientific foundations. Lippincott-Raven, Philadelphia, pp 534–555
17. O'Toole SJ, Sharma A, Karamanoukian HL, Holm B, Azizkhan RG, Glick PL (1996) Tracheal ligation does not correct the surfactant deficiency associated with congenital diaphragmatic hernia. J Pediatr Surg 31:546–550
18. Papadakis K, Luks FI, De Paepe ME, Piasecki GJ, Wesselhoeft CW Jr (1997) Fetal lung growth after tracheal ligation is not solely a pressure phenomenon. J Pediatr Surg 32:347–351
19. Rahier J, Stevens M, De Menten Y, Henquin J-C (1989) Determination of antigen concentration in tissue sections by immunodensitometry. Lab Invest 61:357–363
20. Snyder JM, Magliato SA (1991) An ultrastructural morphometric analysis of rabbit fetal lung type II cell differentiation in vivo. Anat Rec 229:73–85
21. Suen HC, Catlin EA, Ryan DP, Wain JC, Donahoe PK (1993) Biochemical immaturity of lungs in congenital diaphragmatic hernia. J Pediatr Surg 28: 471–477
22. Voorhout WF, Veenedaal HP, Haagsman TE, Whitsett JA, Van Golde LMG, Geuze HJ (1992) Intracellular processing of pulmonary surfactant protein B in an endosomal/lysosomal compartment. Am J Physiol 263:L479–L486
23. Weibel ER (1979) Stereological methods. (Practical methods for biological morphometry). Academic Press, New York
24. Wigglesworth JS, Desia R, Guerrini P (1981) Fetal lung hypoplasia: biochemical and structural variations and their possible significance. Arch Dis Child 56:606–615
25. Wilson JM, Difiore JW, Peters CA (1993) Experimental fetal ligation prevents the pulmonary hypoplasia associated with fetal nephrectomy: Possible application for congenital diaphragmatic hernia. J Pediatr Surg 28:1433–1440